5101-139
Low-Cost
Solar Array Project

DOE/JPL-1012-34
Distribution Category UC-63b

Characterization of Deliberately Nickel-Doped Silicon Wafers and Solar Cells

A.M. Salama

November 1, 1979

Prepared for
U.S. Department of Energy
Through an agreement with
National Aeronautics and Space Administration
by
Jet Propulsion Laboratory
California Institute of Technology
Pasadena, California

(JPL PUBLICATION 79-116)

5101-139
Low-Cost
Solar Array Project

DOE/JPL-1012-34
Distribution Category UC-63b

Characterization of Deliberately Nickel-Doped Silicon Wafers and Solar Cells

A.M. Salama

November 1, 1979

Prepared for
U.S. Department of Energy
Through an agreement with
National Aeronautics and Space Administration
by
Jet Propulsion Laboratory
California Institute of Technology
Pasadena, California

(JPL PUBLICATION 79-116)

Prepared by the Jet Propulsion Laboratory, California Institute of Technology, for the Department of Energy through an agreement with the National Aeronautics and Space Administration.

The JPL Low-Cost Solar Array Project is sponsored by the Department of Energy (DOE) and forms part of the Solar Photovoltaic Conversion Program to initiate a major effort toward the development of low-cost solar arrays.

ACKNOWLEDGMENT

The author wishes to thank the Materials Research Inc. staff for services performed during the course of this evaluation. Special thanks are extended to L. J. Cheng for the use of his facilities for carrying out I-V measurements.

ABSTRACT

Microstructural and electrical evaluation tests were performed on nickel-doped p-type silicon wafers before and after solar cell fabrication. The concentration levels of nickel in silicon were 5×10^{14}, 4×10^{15}, and 8×10^{15} atoms/cm^3. It was found that nickel precipitated out during the growth process in all three ingots. Clumps of precipitates, some of which exhibited star shape, were present at different depths. If the clumps are distributed at depths ~20 μm apart and if they are larger than 10 μm in diameter, degradation occurs in solar cell electrical properties and cell conversion efficiency. The larger the size of the precipitate clump, the greater the degradation in solar cell efficiency. A large grain boundary around the cell effective area acted as a gettering center for the precipitates and impurities and caused improvement in solar cell efficiency. Details of the evaluation test results are given.

CONTENTS

I. INTRODUCTION ---------- 1

A. THE ROLE OF NICKEL IMPURITIES IN SILICON ---------- 1

B. DESCRIPTION OF SILICON WAFERS AND CELLS UNDER INVESTIGATION ---------- 2

II. EXPERIMENTS AND RESULTS ---------- 3

A. MICROSTRUCTURAL EXALUATION OF AS-GROWN SILICON WAFERS ---------- 3

1. Transmission X-Ray Topography ---------- 3

2. Infrared Microscopy ---------- 3

B. MICROSTRUCTURAL EVALUATION OF WAFERS AND SOLAR CELLS AFTER PROCESSING ---------- 10

1. Scanning Electron Microscopy (SEM)/Electron Beam Induced Current (EBIC) ---------- 10

2. X-Ray Topography ---------- 10

3. Optical Microscopy ---------- 10

C. ELECTRICAL EVALUATION OF NICKEL-DOPED SILICON SOLAR CELLS ---------- 14

III. CONCLUSIONS ---------- 17

REFERENCES ---------- 19

Figures

1. (220) X-Ray Topograph of Nickel-doped Silicon Wafer (Concentration 5 x 10^{14} atoms/cm^3) ---------- 4

2. (220) X-Ray Topograph of Nickel-doped Silicon Wafer (Concentration 4 x 10^{15} atoms/cm^3) ---------- 5

3. (220) X-Ray Topograph of Multicrystal Nickel-doped Silicon Wafer (Concentration 8 x 10^{15} atoms/cm^3) ---------- 6

4. Infrared Transmission Photomicrograph of Nickel-doped Silicon Wafer (Concentration 5 x 10^{14} atoms/cm^3) ---------- 7

5. Infrared Transmission Photomicrograph Showing Star-shaped Clumps of Precipitates in Nickel-doped Wafer (Concentration 4 x 10^{15} atoms/cm^3) -------- 8

6. Infrared Transmission Photomicrograph Showing Clumps of Precipitates Aligned along Grain Boundary in Nickel-doped Multicrystal Wafer ---------- 9

7. Scanning Electron Microscope/EBIC Micrograph Showing Electrically Active Star-shaped Precipitate Clump ---------- 11

8. Overview Mosaic Photograph of Multicrystal Nickel-doped Silicon Wafer ---------- 12

9. Photomicrograph of Part of a Sirtl-etched Nickel-doped Silicon Solar Cell ---------- 13

10. Dark Forward I-V Characteristics ---------- 15

Table

1. Illuminated I-V Measurements for Nickel-doped Silicon Solar Cells ---------- 14

SECTION I

INTRODUCTION

During the course of recent studies (Reference 1), it was found that deliberately nickel-doped N^+/P silicon solar cells fabricated from Czochralski-grown single and multicrystal wafers with nickel concentration levels of 5×10^{14} and 8×10^{15} atoms/cm^3, respectively, exhibited conversion efficiencies of 96.3 percent and 93.7 percent of that of the baseline cells. However, deliberately nickel-doped single-crystal solar cells from another ingot but with a nickel concentration level of 4×10^{15} atoms/cm^3, showed a conversion efficiency of 83.2 percent of that of the baseline cells. Nickel concentration levels were determined by neutron activation analysis.

To investigate this discrepancy in results, the nickel-doped silicon wafers and solar cells, cut and fabricated from the three different ingots, were characterized microscopically and electrically. Some of the experiments performed and their results are discussed in this paper.

It was found that nickel precipitated out during the growth process in all three ingots. In the multicrystal ingot with nickel concentration of 8×10^{15} atoms/cm^3, the nickel precipitated along the grain boundaries. The single crystal ingot with nickel concentration of 4×10^{15} atoms/cm^3 exhibited the highest dislocation and precipitate density of the three ingots. These results give evidence of the relationship of structural defects together with concentrations of impurities to solar cell performance.

The microstructural tests performed in this work together with the dark and illuminated I-V measurements and charge collection microscopy measurements make it possible to define the mechanism by which nickel impurities and the other induced crystallographic defects such as grain boundaries, dislocations, and precipitates improve or degrade solar cell performance.

A. THE ROLE OF NICKEL IMPURITIES IN SILICON

Since silicon has a very open diamond lattice structure, atomic diffusion is considerably easier than in a close-packed lattice structure. If there is a distribution of a particular impurity between interstitial and substitutional sites, the effective diffusion coefficient is given by a weighted combination of the two individual diffusion coefficients D_i and D_s (Reference 2):

$$D_{eff} = D_i f + D_s (1 - f) \qquad [1]$$

where f is a fraction in interstitial sites.

It has been found that nickel diffuses predominantly by an interstitial-substitutional mechanism into the silicon lattice (References 3, 4). It has also been reported that substitutional nickel acts as an acceptor in silicon whereas interstitial nickel is electrically inactive, and that most of the dissolved nickel in silicon occupies the interstitial sites (Reference 5). In the present work, by means of electron spin resonance (ESR) measurements, it was found that nickel diffused interstitially in silicon (Reference 6).

In silicon, nickel has a high solubility which is retrograde in character and peaks at ~ 5 x 10^{17} atoms/cm^3 at 2160°C (Reference 7). This causes supersaturation and the formation of precipitates along dislocations and grain boundaries upon cooling after the crystal growth process.

The quality of the p-n junction of the solar cell is intimately related to the structural perfection of the junction depletion region. Crystal growth and device processing steps both introduce into the silicon structural imperfections such as precipitates and dislocations. These structural imperfections provide traps capable of storing and immobilizing the charge carriers. The presence of large grain sizes may enhance cell efficiency, as was found in the case of copper impurities in polycrystalline solar cells (Reference 8). Accordingly, degradation or improvement of electrical behavior of solar cells might occur. Basically, structural defects may affect the electrical behavior of a solar cell in the following ways:

(1) Decrease reverse voltage

(2) Increase reverse current

(3) Decrease minority carrier lifetime

(4) Decrease power output and fill factor, and degrade solar cell efficiency.

The type of adverse electrical behavior is determined by the type, the size, and the distribution of defects.

B. DESCRIPTION OF SILICON WAFERS AND CELLS UNDER INVESTIGATION

Silicon wafers 0.025 cm thick and 3.12 cm in diameter were cut into 1 x 2 cm^2 shapes from ingots prepared by the Czochralski technique with <111> growth axis (Reference 1). Nickel impurities were added to the ingots during the melting process at 1412°C. The molten silicon was boron-doped to a concentration of ~ 10^{16} atoms/cm^3. The cut wafers were chemically polished before the microscopic evaluation.

Solar cells of area 1 x 1 cm^2 were fabricated from the corresponding nickel-doped silicon wafers. The diffusion process was performed at 825°C for 30 minutes, using $POCl_3$ as the phosphorus source; the wafers were cooled immediately to ambient temperature. The junction depth was ~0.4 μm. Thin films of Ti/Pd/Ag metallization were evaporated on the diffused silicon wafers (Reference 1).

SECTION II

EXPERIMENTS AND RESULTS

A set of nondestructive experiments was performed on the as-grown nickel-doped silicon wafers before and after phosphorus diffusion. Another set of experiments was performed on the solar cells to determine the perfection of the junction. The results of the two sets of experiments before and after processing were compared to relate the microstructural defects to the electrical properties of the solar cells.

A. MICROSTRUCTURAL EXALUATION OF AS-GROWN SILICON WAFERS

1. Transmission X-Ray Topography

Silicon wafers of <111> crystal orientation were examined using the nondestructive Lang transmission x-ray method. The (220) topographs of nickel-doped silicon wafers with nickel concentration levels of 5×10^{14}, 4×10^{15}, and 8×10^{15}, atoms/cm^3 are shown in Figures 1, 2, and 3, respectively. The bright spots in the three figures are precipitates present in the wafers. The average dislocation density and precipitate density shown in Figure 1 are ~500 d/cm^2 and 400 P/cm^2, respectively, which are the lowest average densities among the three samples. Figure 2 shows an average dislocation density of 1.5×10^3 d/cm^2 and a precipitate density of 1.5×10^3 P/cm^2. In Figure 3 only one crystal of the multicrystal wafer is shown with precipitates aligned along the boundary. The average dislocation and precipitate densities in this wafer are 500 d/cm^2 and 800 P/cm^2, respectively.

2. Infrared Microscopy

Figures 4, 5 and 6 show transmission infrared photomicrographs for the above-mentioned nickel-doped sample wafers. Figure 4 shows a sample with a nickel concentration of 5×10^{14} atoms/cm^3. As seen in the figure, clumps of precipitates, some exhibiting star shape, are present at different depths varying from 20 μm, 100 μm, 200 μm, and occasionally on the back surface of the wafer. The average clump size is about 12 μm. Figure 5, representing wafers with nickel concentration of 4×10^{15} atoms/cm^3, shows linear arrays of the precipitate clumps. Some of these clumps have star shapes of an average size of ~17 μm. These samples showed a higher precipitate density. The precipitate clumps were closely spaced at different depths varying between 20, 50, 90, 180, and 200 μm below the surface. Figure 6 representing the multicrystal wafer with nickel concentration of 8×10^{15} atoms/cm^3, shows how the precipitates are aligned along the grain boundary. The precipitate average size is ~5 μm.

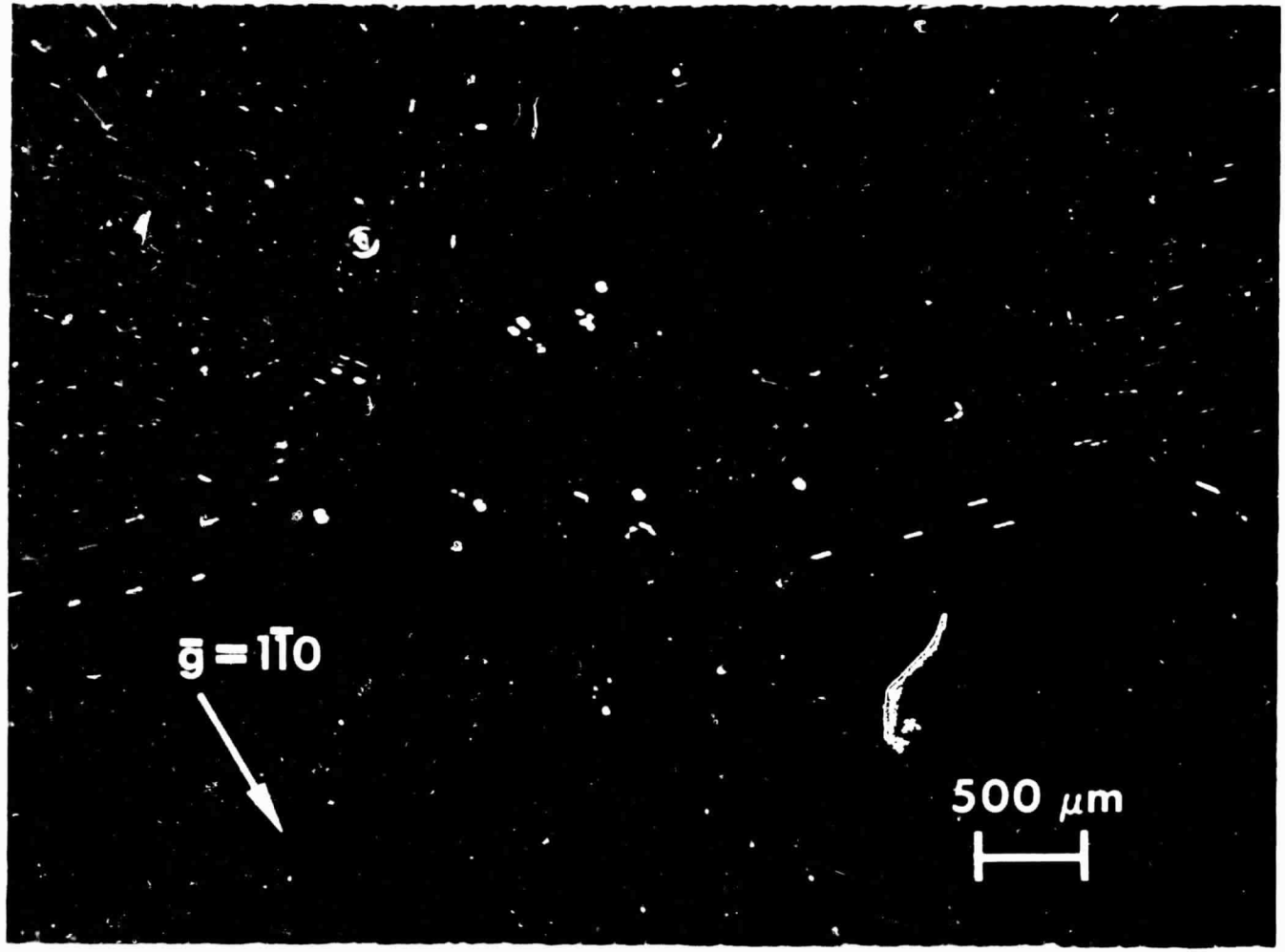

Figure 1. (220) X-Ray Topograph of Nickel-doped Silicon Wafer (Concentration 5×10^{14} atoms/cm^3)

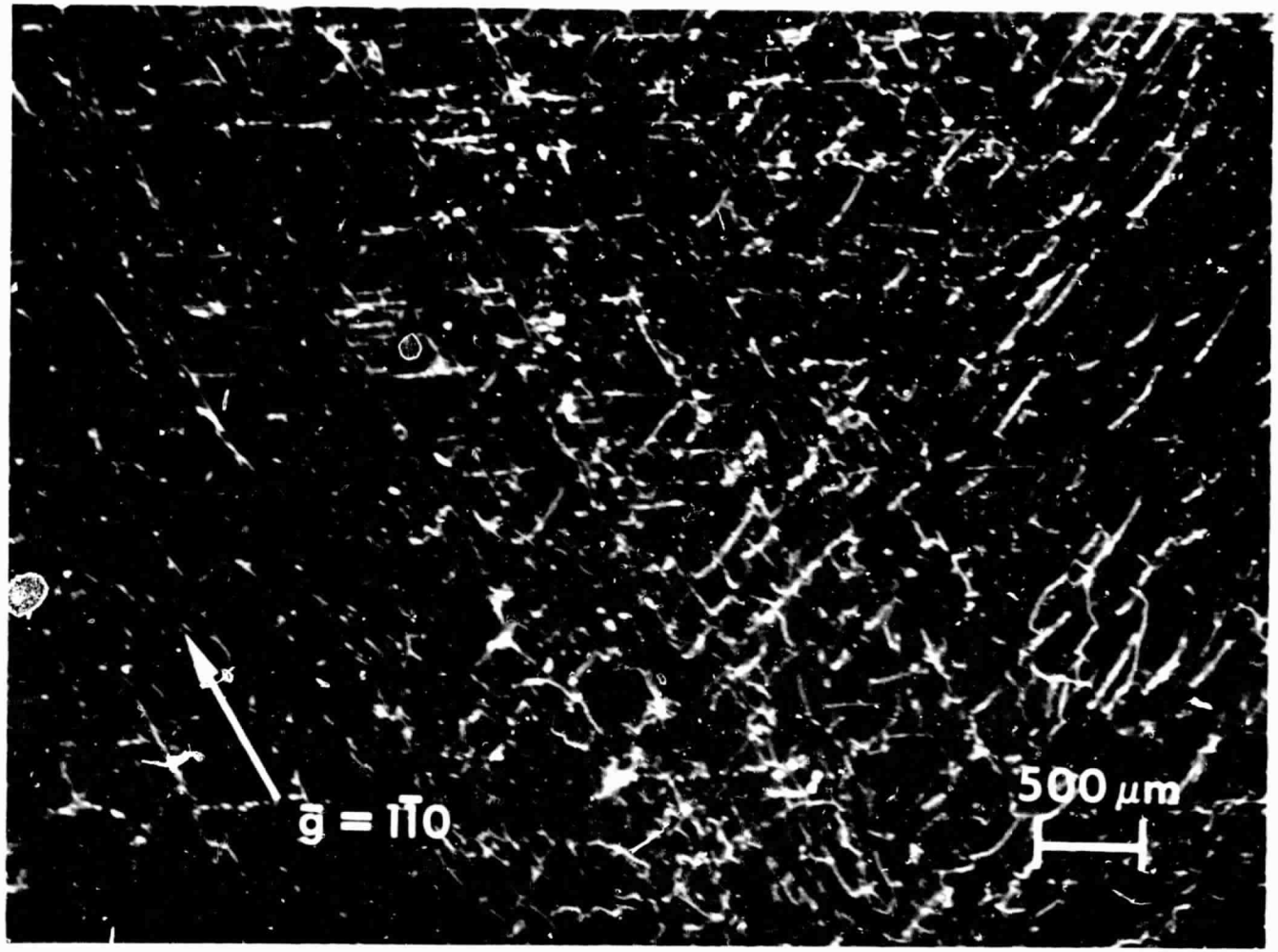

Figure 2. (220) X-Ray Topograph of Nickel-doped Silicon Wafer (Concentration 4 x 10^{15} atoms/cm^3)

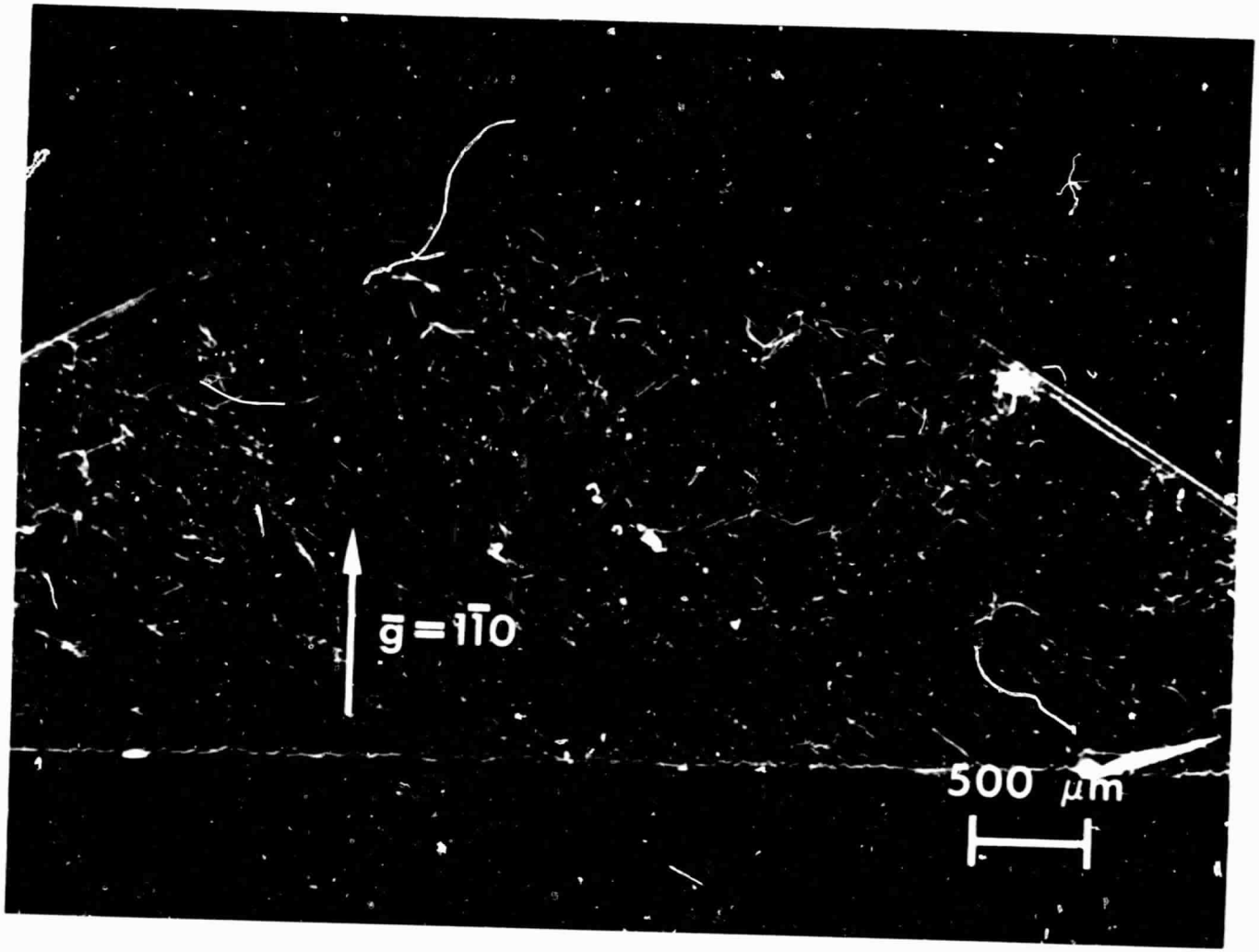

Figure 3. (220) X-Ray Topograph of Multicrystal Nickel-doped Silicon Wafer (Concentration 8×10^{15} atoms/cm^3)

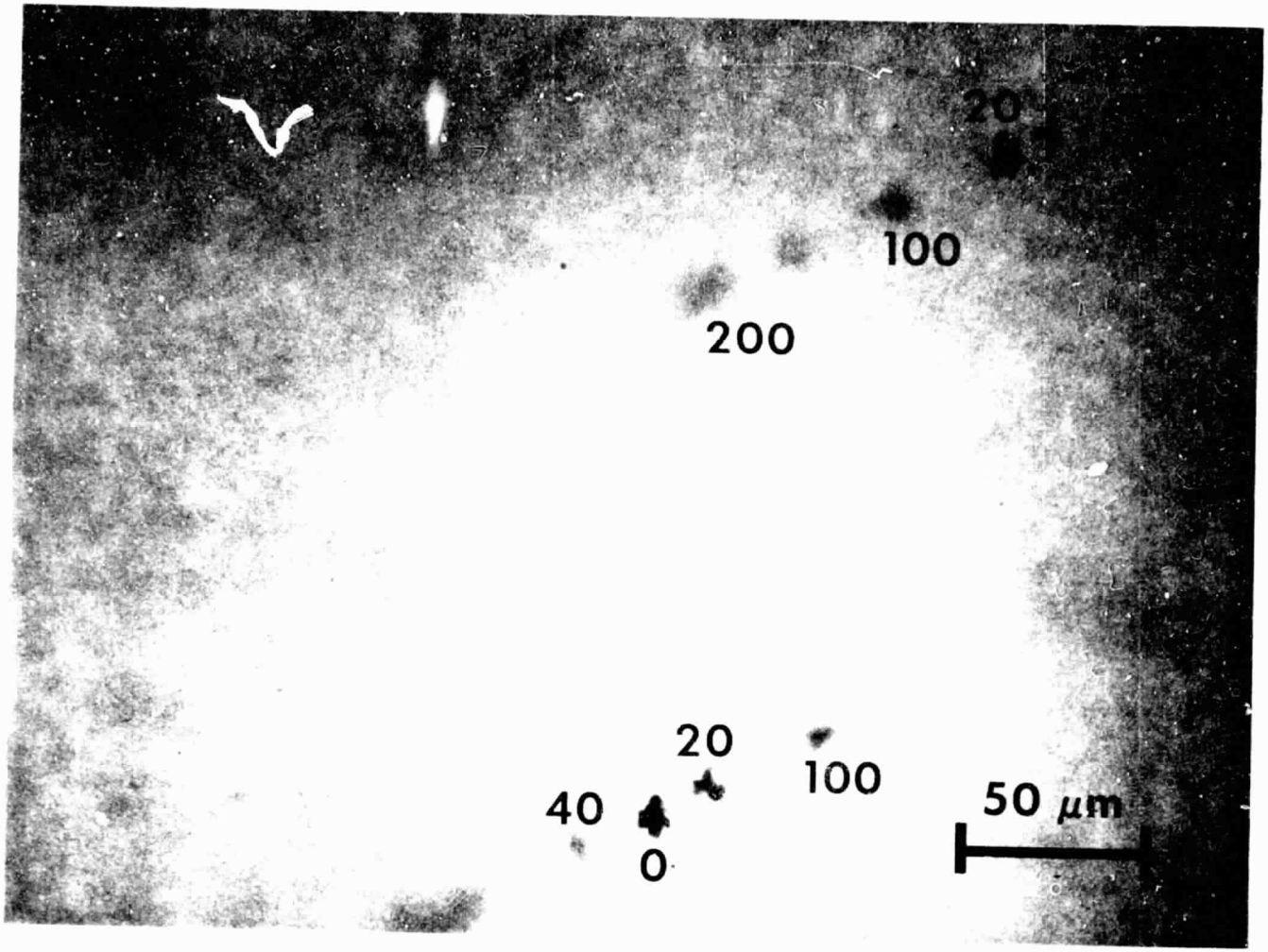

Figure 4. Infrared Transmission Photomicrograph of Nickel-doped Silicon Wafer (Concentration 5×10^{14} atoms/cm^3). Numbers indicate depth of clump in μm from wafer surface

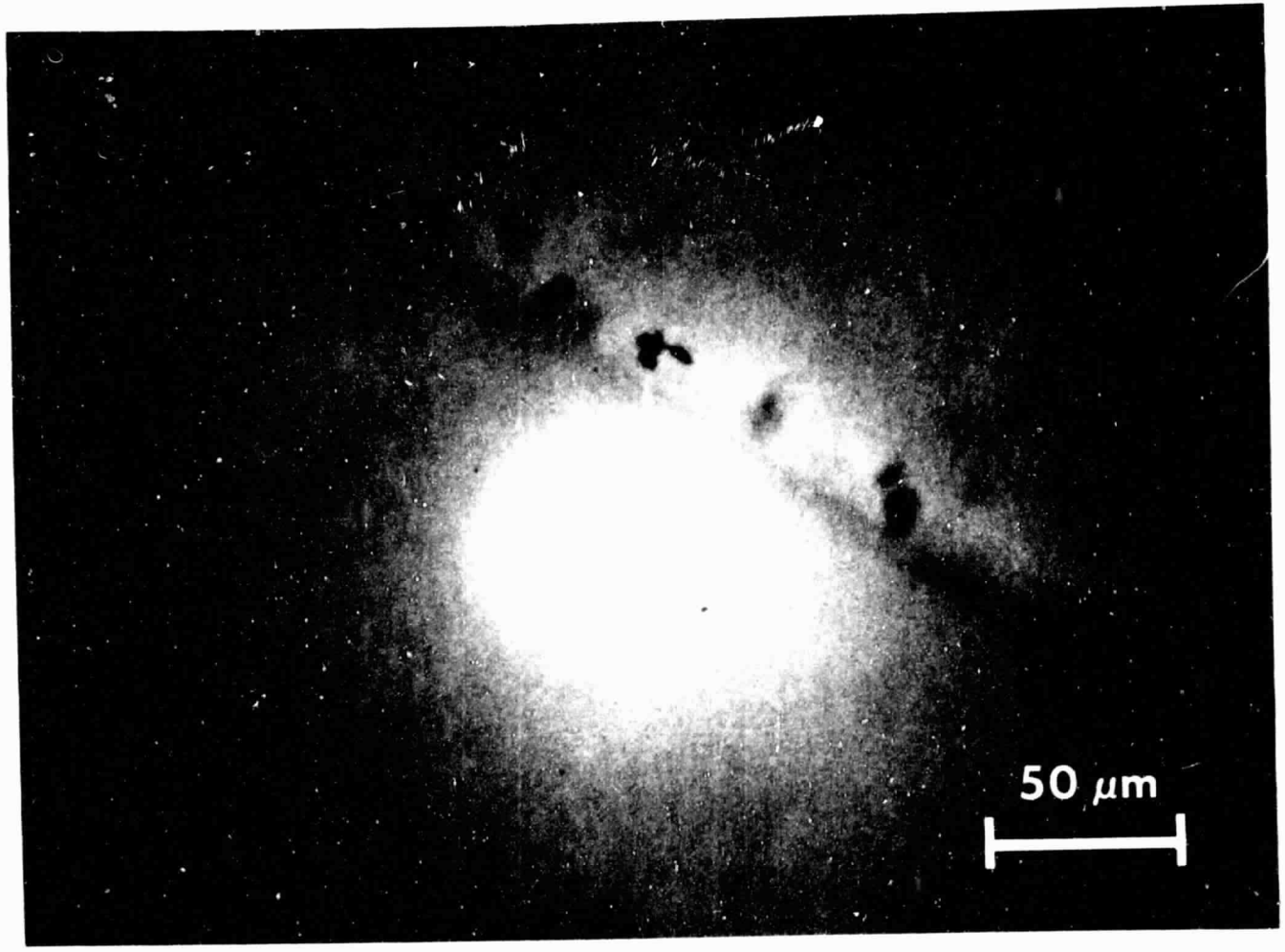

Figure 5. Infrared Transmission Photomicrograph Showing Star-shaped Clumps of Precipitates in Nickel-doped Wafer (Concentration 4×10^{15} atoms/cm^3). Numbers indicate depth of clump in μm from wafer surface

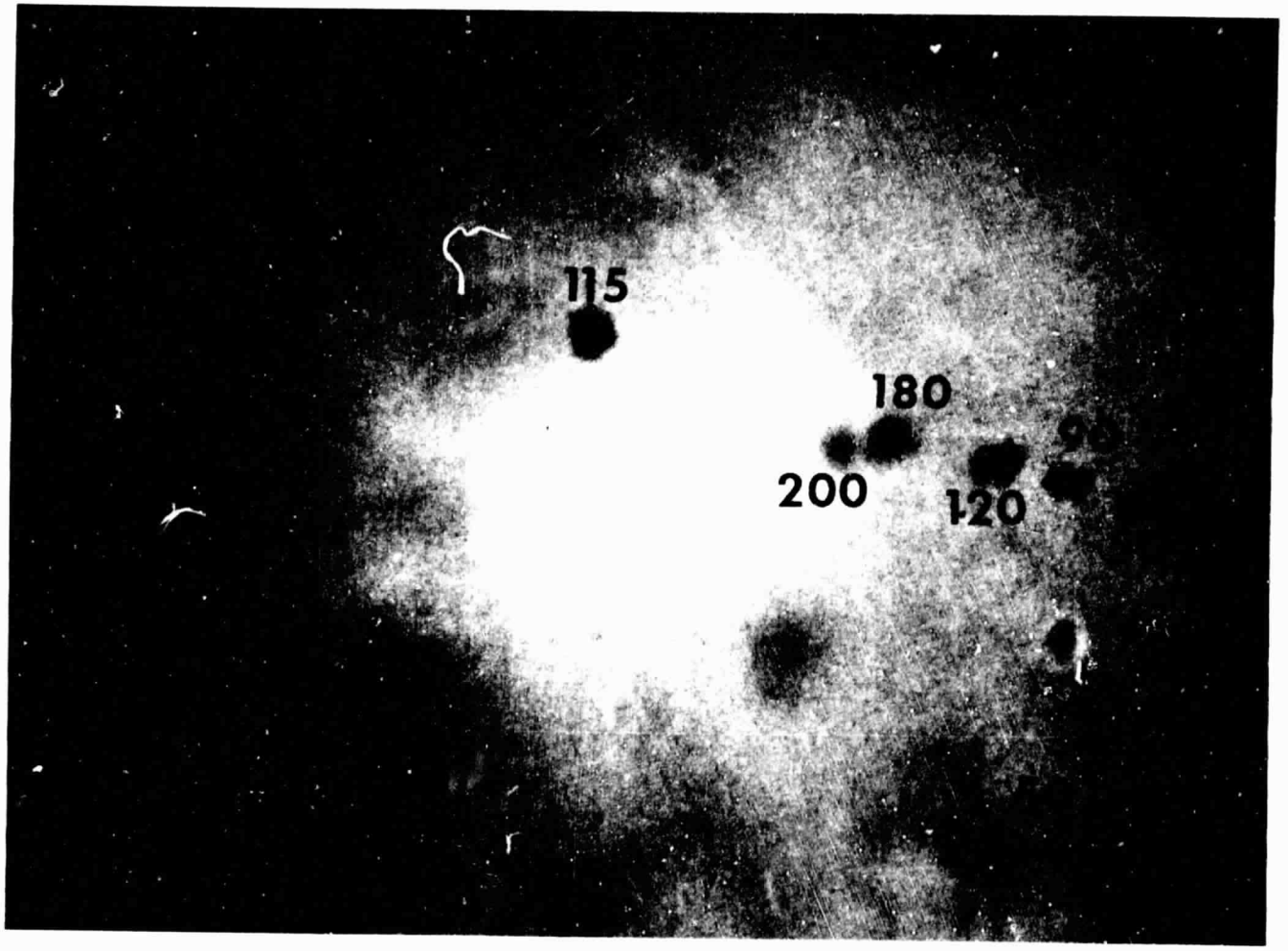

Figure 6. Infrared Transmission Photomicrograph Showing Clumps of Precipitates Aligned along Grain Boundary in Nickel-doped Multicrystal Wafer

B. MICROSTRUCTURAL EVALUATION OF WAFERS AND SOLAR CELLS AFTER PROCESSING

1. Scanning Electron Microscopy (SEM)/Electron Beam Induced Current (EBIC)

This technique was employed on solar cells incorporating the nickel impurities of interest in order to examine the electrically active microstructural defects in the p-n junction depletion region. The scanning electron microscope was operated at ~10 keV, where the electron beam penetration depth is ~0.5 μm, giving an image of the p-n junction depletion region. Figure 7 shows an electrically active clump of precipitate which has a star shape. This defect was typically found in the solar cell with nickel concentration of 5×10^{14} atoms/cm^3. As will be shown later, the presence of these defects caused recombination effects in the junction region. No other electrically active defects were detected in the other nickel-doped solar cells. Figure 8 shows an overview of the solar cell area with nickel concentration of 8×10^{15} atoms/cm^3, where the grain boundary (g.b.) of the multicrystal wafer is seen cutting the cell at one corner. This photomicrograph was taken using the SEM in the secondary emission mode. As expected, the nickel precipitates and impurities were segregated along the boundaries, which in the present case acted as gettering centers for these impurities. Thus, the impurities were gettered away from the cell effective area, except near the cell corner where an ~3.1 mm edge of the grain boundary cut through the cell. This result explains why these cells had good electrical characteristics when compared with the other cells in spite of the fact that they had the highest concentration of nickel.

2. X-Ray Topography

After phosphorus diffusion, Lang transmission x-ray topographs were taken of the samples under investigation. All the topographs showed the appearance of new precipitates and dissolution of some old ones.

3. Optical Microscopy

Figure 9 shows a part of a Sirtl-etched nickel-doped silicon solar cell, with nickel concentration of 5×10^{14} atoms/cm^3. The cell was etched for about 12 seconds (at a depth of ~0.2 μm) in the n^+ region of the junction. As depicted in the photomicrograph, some precipitate clumps appear in linear formations. This indicates that some of the nickel was gettered to the n^+ region of the junction during the phosphorus diffusion process. However, the large clumps of precipitates were not gettered as shown in Figure 7 of the solar cell with nickel concentration of 4×10^{15} atoms/cm^3.

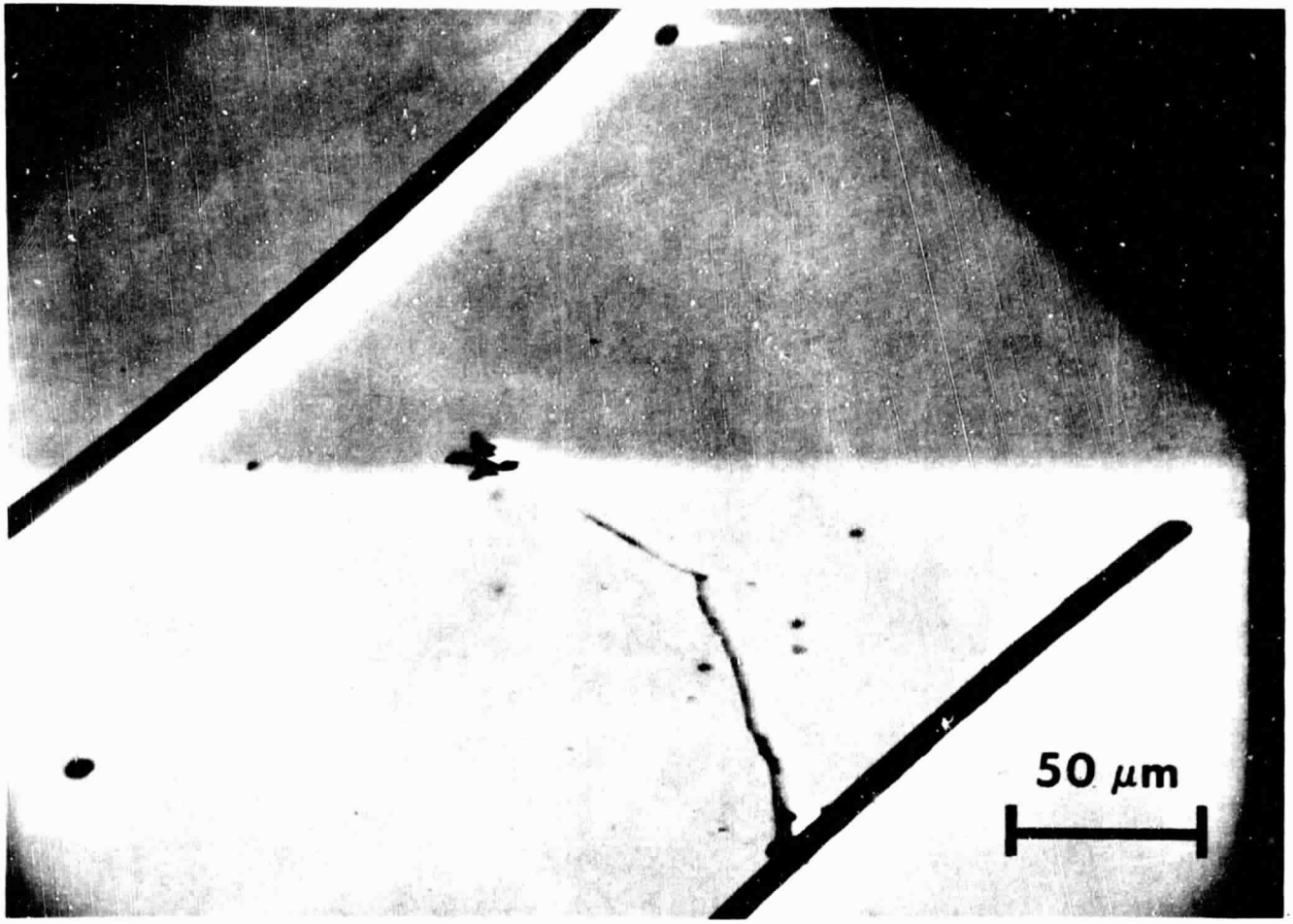

Figure 7. Scanning Electron Microscope/EBIC Micrograph Showing Electrically Active Star-shaped Precipitate Clump

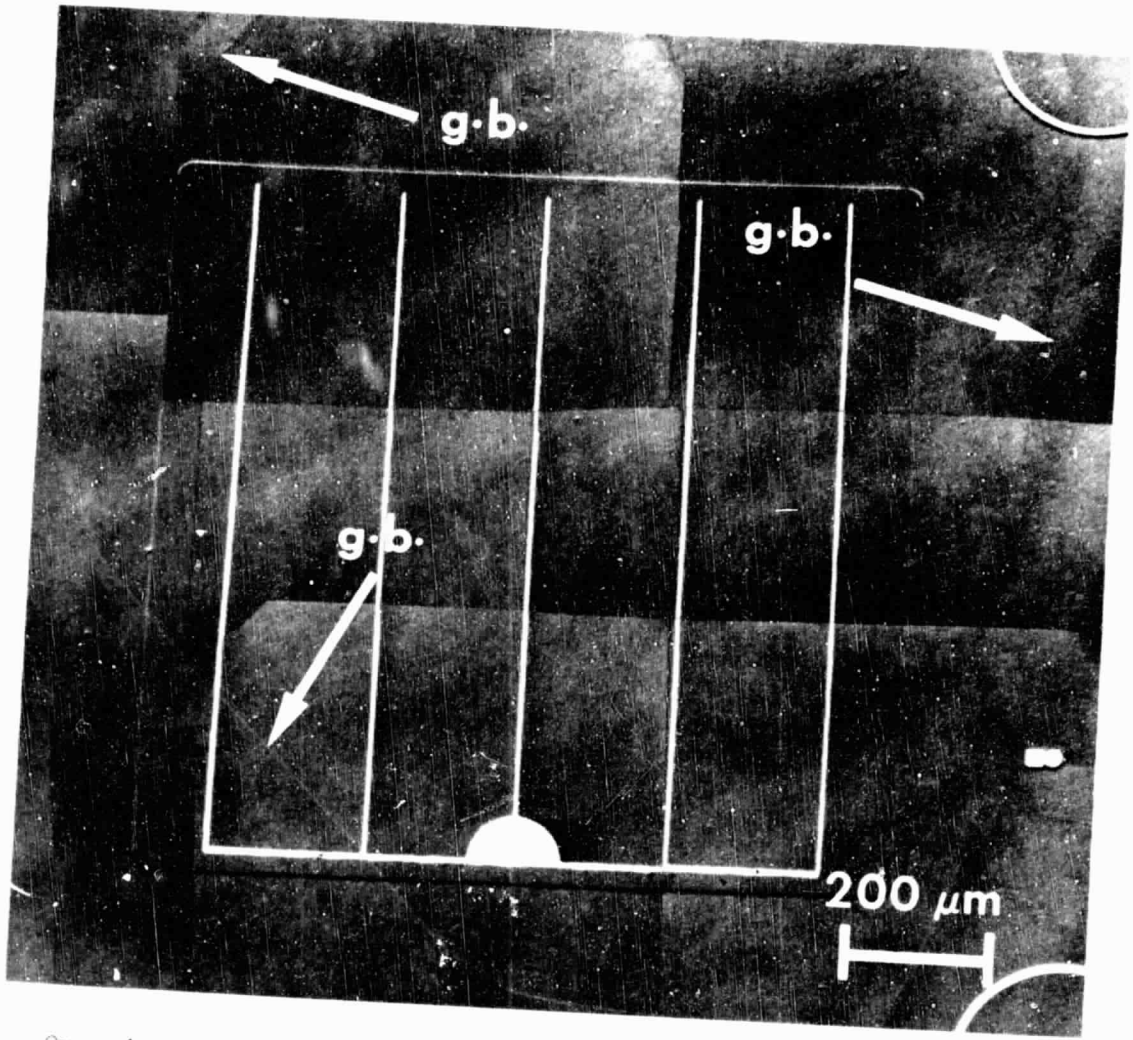

Figure 8. Overview Mosaic Photograph of Multicrystal Nickel-doped Silicon Wafer

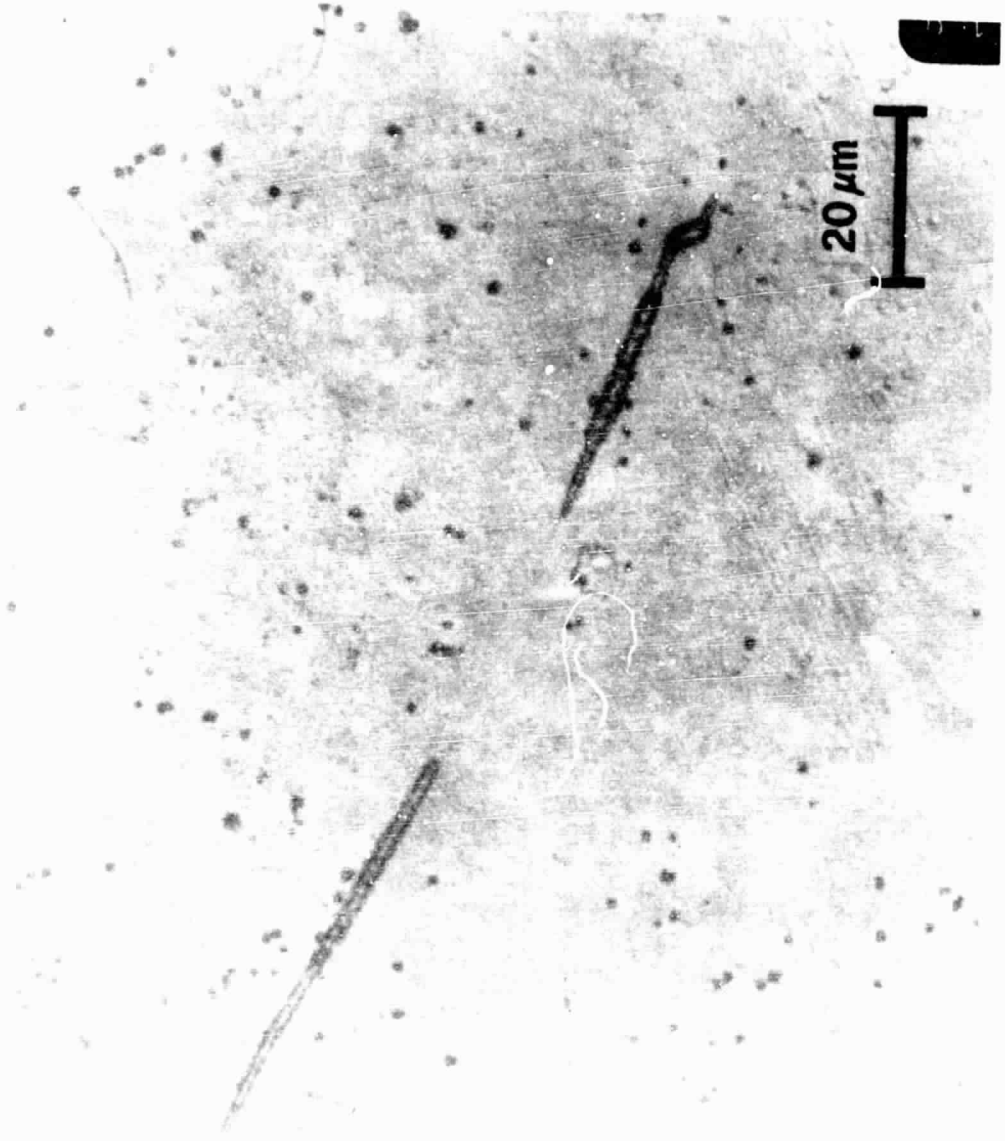

Figure 9. Photomicrograph of Part of a Sirtl-etched Nickel-doped Silicon Solar Cell

C. ELECTRICAL EVALUATION OF NICKEL-DOPED SILICON SOLAR CELLS

Dark forward and reverse biased I-V measurements were performed on nickel-doped silicon solar cells with three different nickel concentration levels. The illuminated I-V measurements (Reference 1) are given in Table 1. These results were correlated with the electrically active microstructural defects observed in the SEM experiment. Figure 10 shows the dark forward I-V characteristics for solar cells with different nickel concentrations. The solar cells with nickel concentrations of 5×10^{14} and 4×10^{15} atoms/cm^3 showed current leakages. They also exhibited considerable deviation of junction perfection factors A_1 and A_2 from the ideal values of 1.0 and 2.0, respectively. Deviation in the A_2 value ($A_2 = 2.6$) is due to recombination of electrical charges at the precipitate clumps, as verified by the SEM/EBIC results shown in Figure 7. The current leakages are due to the presence of closely spaced arrays of precipitate clumps in the bulk of the cells. However, the multicrystal cell with nickel concentration of 8×10^{15} atoms/cm^3 had near ideal A_1 and A_2 factors as seen in Figure 10.

Table 1. Illuminated I-V Measurements for Nickel-Doped Silicon Solar Cells*

Cell ID No.	I_{SC} mA	V_{OC} V	P_{max} W	Efficiency η	Fill Factor	Ni Conc. Atoms/cm^3	% of Baseline η	Remarks
Ni-001 (average)	22.11	0.540	20.41	9.59	0.759	5×10^{14}	96.3	Single crystal
Base-002	22.49	0.549	20.80	9.96	0.763	--	--	
Ni-002 (average)	19.11	0.528	17.67	8.07	0.756	4×10^{15}	83.2	Single crystal
Base-003	22.12	0.552	20.17	9.70	0.751	--	--	
Ni-003 (average)	21.95	0.548	20.09	9.65	0.758	8×10^{15}	93.7	Multi-crystal
Base-020	22.63	0.555	20.39	10.30	0.776	--	--	

*Derived from values published in Reference 1.

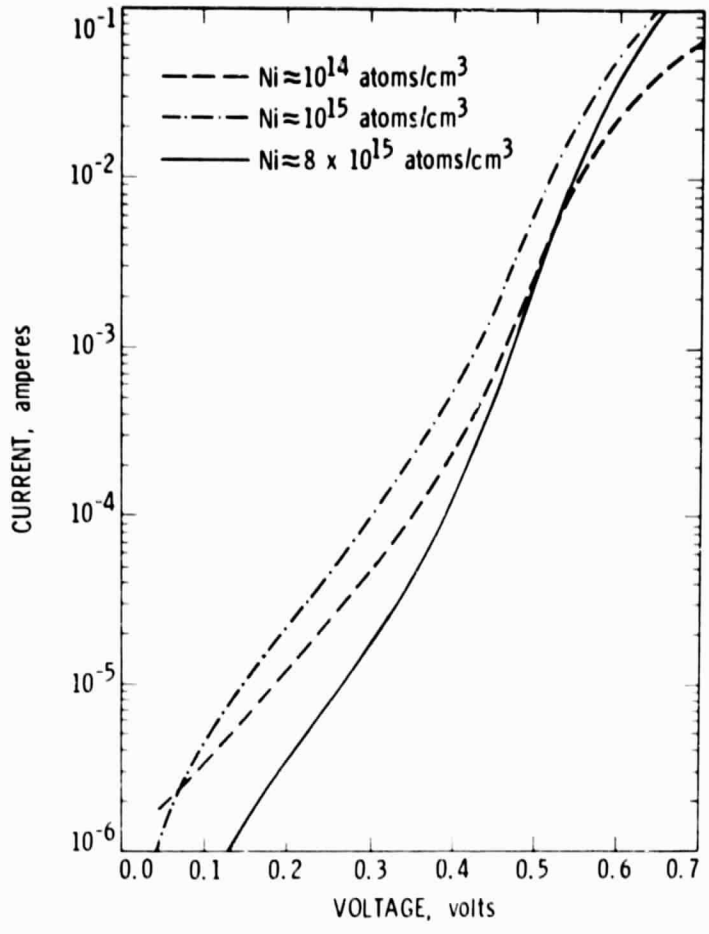

Figure 10. Dark Forward I-V Characteristics

SECTION III

CONCLUSIONS

The results of these studies indicate that the nickel-doped silicon solar cell junction property and electrical behavior are directly related to the size and distribution of microstructural defects such as precipitates, dislocations, and grain boundaries in the cell depletion region and the bulk. Nickel occupies interstitial sites in silicon and precipitates out during the crystal growth process due to its high solubility and diffusivity in silicon.

Furthermore, nickel in concentrations $\geq 4 \times 10^{15}$ atoms/cm^3 caused slight recombination effects, due to the presence of precipitated clumps in the junction depletion region. Current leakage effects are caused by the presence of precipitate clumps if the clumps are distributed at depths ~20 μm apart and are larger than ~10 μm in diameter. The smaller the size of the precipitate clump, the easier it can be gettered out to the n^+ region of the junction during the phosphorus diffusion process. On the other hand, the larger the size of the precipitate clump, the greater the degradation in solar cell efficiency.

Grain boundaries around the cell effective area appear to act as gettering centers for the nickel precipitates and impurities, thus causing improvement in cell efficiencies when the nickel concentration is 8×10^{15} atoms/cm^3. It is noteworthy that this result does not indicate that polycrystalline nickel-doped silicon solar cells are more efficient than single-crystal nickel-doped cells. The polycrystalline cell efficiency depends on the grain sizes and the location of grain boundaries in the cell. On the other hand, the higher the dislocation density, the greater the degradation of the cell electrical properties. Therefore, it appears that large grain sizes enhance the efficiency of nickel-doped silicon solar cells.

REFERENCES

1. Hopkins, R. H., Davis, J. R., Rai-Choudhury, P. and P. D. Blais, Fifth Quarterly Report of Low-Cost Solar Array Project Silicon Material Task, JPL/DOE Contract No. 954331, Westinghouse Research Laboratories, Pittsburgh, PA, December 1976.

2. Kendall, D. L. and B. D. DeVries, "Diffusion in Silicon," Semiconductor Silicon Symposium, Electrochemical Society, Princeton, N. J., 1969.

3. Yoshida, M. and K. Saito, Jap. J. Appl. Phys., 6:573, 1967.

4. Bonzel, H. P., Phys. Stat. Sol., 20:493, 1967.

5. Yoshida, M. and K. Furushi, Jap. J. Appl. Phys., 3:521, 1964.

6. Tsay, F., Jet Propulsion Laboratory, Private Communication (to be published).

7. Aalberts, J. H. and M. L. Verheijke, Appl. Phys. Lett., 1, No. 1:19, 1962.

8. Daud, T. and K. M. Koliwad, Proceedings of the Thirteenth IEEE Photovoltaic Specialists Conference, Washington, D.C., June 1978.